



Published in final edited form as:

Oncogene. 2013 May 2; 32(18): . doi:10.1038/onc.2012.243.

The Hedgehog processing pathway is required for NSCLC growth and survival

Jezabel Rodriguez-Blanco^{1,*}, Neal S. Schilling^{1,9,*}, Robert Tokhunts^{1,9}, Camilla Giambelli¹, Jun Long¹, Dennis Liang Fei^{1,9}, Samer Singh¹, Kendall E. Black¹, Zhiqiang Wang¹, Fabrizio Galimberti⁹, Pablo A. Bejarano⁴, Sharon Elliot⁵, Marilyn K. Glassberg⁶, Dao M. Nguyen^{1,2}, William W. Lockwood⁷, Wan L. Lam⁸, Ethan Dmitrovsky^{9,10}, Anthony J. Capobianco^{1,2}, and David J. Robbins^{1,2,3}

¹Molecular Oncology Program, Department of Surgery, University of Miami, Miami, 33136, FL, USA

²Sylvester Cancer Center, Miller School of Medicine, University of Miami, Miami, 33136, FL, USA

³Department of Biochemistry and Molecular Biology, University of Miami, Miami, 33136, FL, USA

⁴Department of Pathology, University of Miami, Miami, 33136, FL, USA

⁵Laboratory on Sex and Gender Differences in Health and Disease, Department of Surgery, University of Miami, Miami, 33136, FL, USA

⁶Pulmonary and Critical Care Medicine, Department of Medicine and Department of Surgery, Jackson Memorial Hospital, University of Miami, Miami, 33136, FL, USA

⁷Cancer Genetics Branch, National Human Genome Research Institute, Bethesda, 20892, MD, USA

⁸Department of Integrative Biology, British Columbia Cancer Research Centre, Vancouver, BC, V5Z1L3, Canada

⁹Department of Pharmacology and Toxicology, Dartmouth Medical School, Hanover, , NH, USA

¹⁰Norris Cotton Cancer Center, Dartmouth Medical School and Dartmouth-Hitchcock Medical Center, Lebanon, 03755, NH, USA

Abstract

Considerable interest has been generated from the results of recent clinical trials using SMOOTHENED (SMO) antagonists to inhibit the growth of HEDGEHOG (HH) signaling dependent tumors. This interest is tempered by the discovery of SMO mutations mediating resistance, underscoring the rationale for developing therapeutic strategies that interrupt HH signaling at levels distinct from those inhibiting SMO function. Here, we demonstrate that HH dependent non-small cell lung carcinoma (NSCLC) growth is sensitive to blockade of the HH pathway upstream of SMO, at the level of HH ligand processing. Individually, the use of different lentivirally delivered shRNA constructs targeting two functionally distinct HH-processing proteins, SKINNY HEDGEHOG (SKN) or DISPATCHED-1 (DISP-1), in NSCLC cell lines

Corresponding Author: David J. Robbins Ph.D., Professor of Surgery and Professor of Biochemistry and Molecular Biology, Miller School of Medicine, University of Miami, 1042 RMSB, 1600 NW 10th Avenue, Miami, FL 33136. Phone: 305-243-5717; Fax: 305-243-2810; drobbins@med.miami.edu.

*Jezabel Rodriguez-Blanco and Neal Schilling contributed equally to this work.

Conflict of interest

The authors declare no conflict of interest.

Supplementary information is available at ONCOGENE website.

produced similar decreases in cell proliferation and increased cell death. Further, providing either an exogenous source of processed HH or a SMO agonist reverses these effects. The attenuation of HH processing, by knocking down either of these gene products, also abrogated tumor growth in mouse xenografts. Finally, we extended these findings to primary clinical specimens, showing that *SKN* is frequently over-expressed in NSCLC and that higher *DISP-1* expression is associated with an unfavorable clinical outcome. Our results show a critical role for HH processing in HH-dependent tumors, identifies two potential druggable targets in the HH pathway, and suggest that similar therapeutic strategies could be explored to treat patients harboring HH ligand dependent cancers.

Keywords

DISPATCHED; Lung Cancer; Hedgehog; HEDGEHOG ACYLTRANSFERASE; SKINNY HEDGEHOG

INTRODUCTION

The HEDGEHOG (HH) family of secreted proteins, consisting of SONIC (SHH), INDIAN and DESERT HH, is broadly active during development as a morphogen, and in adults is critical for the maintenance of a variety of tissues^{1,2}. Consistent with this critical physiological role regulating proliferation, differentiation and apoptosis, aberrant HH signaling is also evident in a large range of human tumors^{3,4}. In such tumors, HH pathway activation results from non-canonical activation of GLI transcription factors, activating mutations in downstream effectors, or from increased expression of HH ligands^{3,4}. HH ligands elicit their effects by binding to their receptor, PATCHED-1 (PTCH-1)^{5,6}, which in turn relieves PTCH-1-mediated repression of SMOOTHENED (SMO)^{7,8}. SMO goes on to activate downstream targets by regulating the levels and processing of the GLI family of transcription factors: GLI-1, GLI-2 and GLI-3^{1,9}. Encouragingly, inhibiting the HH pathway with the SMO antagonist Vismodegib (GDC-0449) has had success in clinical trials as a targeted therapy, and many other SMO antagonists are being studied for activity against various solid tumors¹⁰⁻¹². There are, however, already reports of clinical relapses associated with GDC-0449 refractory SMO mutations, demonstrating a need for alternative, functionally distinct targets in the HH pathway^{13,14}.

HH proteins undergo a series of processing steps prior to the secretion of the fully active protein. Initially these are translated as a ~45 kDa preprotein containing a signal peptide, an amino-terminal domain and a carboxy-terminal domain^{15,16}. As HH traverses the secretory pathway, the carboxy-terminal domain catalyzes an intramolecular cleavage reaction that results in the addition of cholesterol to the newly created carboxy-terminus of the amino-terminal domain¹⁶. The amino-terminus of this is further modified by the addition of a second lipid, palmitate¹⁷, in a reaction catalyzed by the palmitoyl-transferase SKINNY HEDGEHOG (SKN, alternatively called HEDGEHOG ACYLTRANSFERASE)¹⁸⁻²². Palmitoylation of HH is necessary for ligand activity, with various lipid modifications increasing the activity of recombinant SHH 40 to 160-fold^{23,24}. This dual-lipid modified HH is transported to the cell surface where its release is regulated by the activity of DISPATCHED-1 (DISP-1), a 12-pass transmembrane domain protein with homology to RESISTANCE-NODULATION-DIVISION (RND) PERMEASES²⁵. Mice engineered to lack *DISP-1*²⁶⁻²⁸ or *SKN*²⁹ function are embryonic-lethal, and display early embryonic phenotypes reminiscent of *SMO* null mice³⁰. Together, these observations underscore the critical role of HH processing in canonical, ligand-dependent HH signaling.

In non-small cell lung carcinoma (NSCLC), ligand-dependent HH signaling promotes proliferation and tumorigenesis *in vitro* and *in vivo*^{31–34}. We, and others, reported frequent constitutive HH pathway activation in primary human NSCLC tumors; an observation recapitulated in tumors derived from transgenic mice overexpressing *CYCLIN-E* in the lung. We further demonstrated that two shRNA specifically targeting *GLI-1*, but not a scramble control, were able to significantly reduce the growth of NSCLC xenografts *in vivo*³¹, consistent with HH signaling being critical for tumorigenesis. *In vitro*, the expression of HH target genes increased when NSCLC cells were transfected with SHH and decreased when HH ligand expression was knocked down³¹. Together, these results demonstrated that NSCLC cells harbor a functionally intact HH pathway, both producing active ligand and responding to it. Based on this prior work, we hypothesized that blocking HH signaling upstream of SMO would attenuate NSCLC growth. Here, we present results showing that disrupting HH biogenesis reduces NSCLC proliferative capacity *in vitro* and the growth of such tumors *in vivo*. These findings support the autocrine role of HH signaling in NSCLC, and demonstrate the existence of two previously unrecognized druggable targets upstream of SMO.

RESULTS

The HH Acyl-transferase SKN regulates HH activity

To explore a potential role for SKN as a therapeutic target in HH-dependent tumors we isolated its cDNA, and used a plasmid expressing this cDNA to verify its functional role in regulating HH activity. We transfected HEK cells with a plasmid expressing *wtSHH*, or a mutant of SHH in which the palmitate acceptor Cys¹⁷ was mutated to a Ser (*SHHC24S*), with or without a plasmid expressing *SKN*. These cells were subsequently incubated with ³H-palmitate, followed by immunoprecipitation of SHH, separation of these immunoprecipitates by SDS-PAGE and fluorography to determine the degree of SHH palmitoylation. Co-transfection of plasmids expressing *SKN* with *wtSHH*, but not *SHHC24S*, increased the palmitoylation of SHH, confirming the activity of our *SKN* construct (Figure 1a). SHH potency in conditioned media (CM) isolated from HEK cells transfected with a plasmid expressing *wtSHH*, along with different amounts of a plasmid expressing *SKN* or an empty vector control, was measured to estimate changes in SHH activity. These various CMs were assayed using cells that stably express a HH-responsive luciferase reporter construct (SHH-Light2 cells)³⁵. Co-transfection of plasmids expressing *SKN* with *wtSHH* increased the potency of SHH in a dose-dependent manner (Figure 1b), consistent with SKN playing a pivotal role in HH activity.

As a tool to determine the importance of SKN for SHH activity, we next evaluated the ability of distinct *SKN* specific, lentivirally delivered, shRNA to knockdown SKN levels. Knockdown of endogenous SKN protein was confirmed by immunoprecipitating SKN (antibody: SKN2883) from the lysates of H23 cells transduced with *SKN* specific shRNA (Figure 1c), then immunoblotting these immunoprecipitates with a second anti-SKN antibody (antibody: SKN2884). The specificity of these anti-SKN antibodies was validated using a MYC-tagged *SKN* construct (Supplemental Figure S1a–b). The two most active *SKN* shRNAs were evaluated for their ability to knockdown endogenous *SKN* mRNA levels and affect SHH potency in cells that stably express *SHH* (SHH-I cells)³⁶. Knockdown of *SKN* in these cells was verified by quantitative real-time PCR (qRT-PCR) (Figure 1d). When the CM from these transduced cells was assayed with SHH-Light2 cells we observed reduced SHH potency compared to the CM from cells transduced with a virus expressing a scramble control shRNA (Figure 1e). Together, these results validate that SKN palmitoylates SHH²² and that this palmitoylation is a key determinant of SHH activity^{23,24}.

SKN is necessary for the proliferation of NSCLC cells

We previously characterized the critical role HH signaling plays in human and mouse NSCLC cell lines, using two distinct shRNA targeted to numerous positive acting components of the HH signaling pathway, as well as several SMO antagonists, to attenuate their proliferation and tumorigenicity^{31,32}. Consequently, we decided to use these well-characterized NSCLC cell lines to explore the importance of key HH processing regulators to the viability of such HH-dependent cell lines. We individually knocked down *SKN* levels with two different shRNAs in human A549, HOP62, U1752, H23, H522 and murine ED1^{33,37} NSCLC cells, and estimated their proliferation relative to a shScramble control using a Cell Titer-Glo (CTG) assay (Figure 2a–b). We observed a reduction in cellular proliferation upon knocking down *SKN* levels, relative to transduction with control shRNA, and this reduction occurred in all human and mouse NSCLC cell lines tested. To confirm the reduced proliferation observed in the CTG assay we tested BrdU incorporation, a more direct measure of cellular proliferation, in A549 and Hop62 cells transduced with *SKN* specific shRNA. The number of BrdU positive cells observed after reduction of *SKN* levels was significantly decreased compared to the shScramble control (Figure 2c), confirming a decrease in the rate of proliferation. Similar results were obtained using an MTT assay where we further validated our results using three additional negative controls or two extra *SKN* specific shRNAs (Supplemental Figure S2a).

We speculated that decreases in proliferation observed upon reduction of *SKN* levels might in part result from increased cell death. We therefore knocked down *SKN* and measured the release of the cytoplasmic protein lactate dehydrogenase (LDH) into CM, a commonly used indicator of cell death³⁸. Using this assay we observed a significant increase in cell death in response to reduced *SKN* levels, and this increase was observed using two distinct *SKN* specific shRNA in two different NSCLC cell lines (Figure 2d). Moreover, knockdown of *SKN* in A549 cells led to an activation of the apoptosis effector caspase: CASPASE-3, suggesting that the observed cell death is driven by apoptosis (Supplemental Figure S4a). As a more direct measurement of cell viability, we performed a limiting dilution clonal growth assay³⁹. The clonal growth of A549 cells was almost completely abrogated when transduced with *SKN* specific shRNA, but not with a shScramble control (Figure 2e and Supplemental S2b). Taken together, these results indicate that SKN is critical for the proliferation of NSCLC lines and that loss of SKN can result in cell death, consistent with our previous work suggesting that HH signaling has roles in both the proliferation and survival of NSCLC cells^{31,32}.

SKN is required for HH pathway activity in NSCLC cells

As this is the first description of a critical role for HH processing in cancer, we next wanted to determine if the observed cytotoxic/cytostatic effects of *SKN* knockdown were due to inhibition of ligand-dependent HH signaling. To assess HH pathway activity, we examined the expression of two well-accepted HH target genes, *GLI-1* and *PTCH-1*, by qRT-PCR^{1,9}. Knockdown of *SKN* resulted in significant reductions in the expression of *GLI-1* and *PTCH-1* in A549 (Figure 3a) and Hop62 (Figure 3b) cells, relative to cells transduced with a shScramble control. Additionally, ED1 cells selected to stably express one of two distinct *SKN* specific shRNA had significantly lower HH target gene expression compared to ED1 cells stably expressing a shScramble control (Figure 3c). Knockdown of *SKN* in A549 cells also reduced the levels of GLI-1 (Figure 3d) and CYCLIN-D1 proteins (Figure 3e), both of which are commonly used biomarkers of the HH signaling pathway^{1,40}. These results confirm that HH ligand processing also regulates HH pathway activity in NSCLC lines.

DISP-1 is required for NSCLC proliferation, and the oncogenic effect of disrupting ligand processing is HH specific

While SKN function is primarily linked to the function of HH proteins¹⁸, Drosophila SKN also appears to regulate the activity of a palmitoylated form of Epidermal Growth Factor⁴¹. Thus, it remains possible that while SKN can regulate HH activity in NSCLC cells, its effect on the viability of cancer cells might be due to it acting on some other signaling protein. To further demonstrate the importance of HH processing to cancer cell proliferation we examined the role of a second HH processing protein, DISP-1²⁵, in NSCLC viability.

We again used a lentiviral driven approach to knockdown *DISP-1* in NSCLC cell lines. Knockdown of *DISP-1* was observed at the mRNA level (Figure 4a–b), and at the protein level, as determined using a novel DISP-1 specific antibody (Figure 4c, Supplemental Figure S1c). As was observed when knocking down *SKN*, knocking down *DISP-1* with multiple different shRNA resulted in significant reductions in HH target genes in both A549 (Figure 4a) and Hop62 (Figure 4b) cells. Knockdown of *DISP* also abrogated the release of SHH into CM whereas knockdown of *SKN* did not affect SHH secretion (Supplemental Figure S4b), consistent with their respective roles in SHH processing^{23,24,25}.

DISP-1 knockdown was also accompanied by a decreased number of viable cells, as measured by MTT reduction (Supplemental Figure S2a). To again determine if the decrease in cell number observed upon reducing *DISP-1* levels was due to a fall in proliferation we transduced NSCLC cell lines with *DISP-1* specific shRNA and measured BrdU incorporation. Two distinct *DISP-1* shRNA caused a significant reduction in the proliferation of these cancer cell lines (Figure 4d). As we observed with *SKN* knockdown, reduction of *DISP-1* levels also resulted in increased release of LDH into CM (Figure 4e), and cleavage of the apoptosis effector caspase, CASPASE-3 (Supplemental Figure S4a), both of which are consistent with an increase in apoptotic cell death. Additionally, sh*DISP* transduction abrogated the clonogenic growth of A549 cells (Figure 4f and Supplemental Figure S2b). These results were similar to those observed in NSCLC cells following *SKN* knockdown.

To further establish a link between reduced HH processing and the observed cytostatic/cytotoxic effects of inhibiting SKN and DISP-1 function, we used an exogenous source of lipid modified SHH³⁶, reasoning that such a form of SHH would bypass the processing defects of these NSCLC cells. We added purified, lipid modified, SHH to the media of sh*SKN* or sh*DISP* transduced NSCLC cells and then measured their viability. Purified lipid modified SHH was indeed able to rescue cell viability in a statistically significant manner (Figure 4g); however, the presence of the detergent required to keep the lipid modified SHH in solution limited the amount of SHH we could effectively add back to the processing defective NSCLC cells. Despite this limitation significant rescue was observed. We were additionally able to rescue cell viability using the SMO agonist purmorphamine⁴² (Figure 4h). These results are consistent with the attenuated cell viability observed upon knockdown of *SKN* or *DISP-1* being due to a disruption of ligand dependent HH signaling.

HH processing is required for NSCLC growth *in vivo*

We next sought to elucidate the *in vivo* significance of these findings using two distinct mouse models of NSCLC. To explore the role of SKN in a syngeneic FVB mouse model of NSCLC³⁷ we transduced GFP expressing ED1 cells with either a scramble control shRNA or one of two previously validated *SKN* specific shRNA. Although the majority of these cells died, we were able to select surviving polyclonal stable lines that expressed reduced levels of *SKN* (Figure 3c). These cell lines were injected into the tail vein of syngeneic FVB mice. Four weeks later lung tissue was harvested, sectioned and stained for GFP expression.

A blinded investigator then quantified GFP positive lesions. Significantly fewer lesions were observed in the lungs of animals injected with cells expressing reduced levels of *SKN* (Figure 5a).

A second *in vivo* NSCLC model, consisting of transplanting human NSCLC cells into an immunocompromised mouse as a xenograft³¹, was also used to assess the role HH processing plays in human NSCLC. A549 cells were transduced with either a scramble, one of two *SKN* specific, or one of two *DISP-1* specific shRNA. These cells were injected into the flanks of nude mice and tumor volume measured twice weekly for 5 weeks. Tumor formation and histology was verified by H&E staining and was scored by a board certified lung pathologist (Dr. Pablo A. Bejarano, data not shown). The mean tumor volume of A549 xenografts transduced with either *SKN* or *DISP-1* specific shRNA was reduced in a statistically significant manner, compared to cells transduced with a scramble shRNA (Figure 5b–c). These results suggest a critical role for *SKN* and *DISP-1* in NSCLC growth.

HH processing gene products are overexpressed in human NSCLCs and are associated with an unfavorable clinical outcome

To further investigate the role of HH processing in human NSCLC we examined the expression of *SKN* and *DISP-1* in 58 pairs of tumor and matched normal tissue using an oligonucleotide micro-array⁴³. The majority of these patient samples expressed higher levels of *SKN* in the tumor versus the adjacent normal tissue (Figure 6a and Supplemental S3a). A smaller subset of tumors also overexpressed *DISP-1* (Figure 6b). We also directly analyzed the expression of *SKN* and *DISP-1* in a commercially available cDNA array consisting of 24 pairs of matched lung tumor and normal lung tissue. The same patterns of expression of *SKN* and *DISP-1* observed in the micro-array were also abnormal by qRT-PCR analysis (Figure 6c–d). To further confirm these results we again directly analyzed the expression of *SKN* and *DISP-1* in 6 pairs of tumor and matched normal tissue harvested locally by our group (Supplemental Figure S3b). We performed immunohistochemistry on these same samples to determine the levels of SHH, which we then compared with *SKN* and *DISP-1* mRNA expression. Although the sample size was too small to draw any statistical conclusions, tumors with increased *SKN* expression are the ones with the strongest SHH staining (Supplemental Figure S3c).

We mined publically available data sets consisting of tumor micro-array data matched with clinical outcome (overall and progression free survival), in order to assess the clinical significance of *SKN* and *DISP-1* expression. There was no correlation seen between *SKN* expression and clinical outcome (data not shown), however increased *DISP-1* expression correlated with decreased recurrence free and overall survival in the two data sets analyzed (Figure 6 e–f and data not shown). These results point to a critical and clinically relevant role for HH ligand processing in NSCLC tumorigenesis, progression and recurrence.

DISCUSSION

The HH signaling pathway plays a critical role in the growth and maintenance of a wide variety of human tumors^{3,4}. This, coupled with the recent early success of GDC-0449 in clinical trials^{10–12} and our results, indicates that pharmacological inhibition of the HH pathway would be therapeutically beneficial in clinical NSCLC. Indeed, various SMO inhibitors are currently undergoing trials for the treatment of a wide array of solid tumors, including NSCLC^{10,11,44}. There are, however, already reports of drug resistant SMO mutations^{13,14}, highlighting the importance of finding alternative druggable targets within the HH pathway. Considerable work has been focused on the HH pathway downstream of SMO, with compounds having successfully been developed that antagonize GLI transcription factors⁴⁵. Conversely, potential drug targets upstream of SMO have remained,

for the most part, unexplored⁴⁶. We show here that disruption of the HH signaling pathway upstream of SMO, at the level of HH ligand processing, inhibits HH signaling and subsequently attenuates tumorigenesis. As high-level HH activity is dependent on lipid modification^{23,24}, we first disrupted HH processing by reducing the levels of SKN, the enzyme responsible for the amino-terminal palmitoylation of HH^{18,22}. This resulted in reduced HH pathway activity in NSCLC cell lines, as demonstrated by both decreased target gene expression and reduced steady-state levels of two protein biomarkers. Attenuation of HH signaling was accompanied by decreased cell viability *in vitro* and reduced tumor growth in both a xenograph and a syngeneic *in vivo* model of NSCLC. Strikingly, similar effects were observed when levels of the protein required for the release of cholesterol modified HH, DISP-1²⁵ were reduced. Combined, these results suggest that the effects observed upon reducing SKN or DISP-1 levels result from inhibition of HH signaling, as reducing the levels of two otherwise unrelated components of the HH biogenesis pathway decreases NSCLC cell viability. Furthermore, consistent with this decreased cell viability being caused by reduced HH activity, providing these cells with either exogenous dually lipid modified SHH or the SMO agonist purmorphamine resulted in a significant rescue of cell viability.

Both *SKN* and *DISP-1* are located on chromosome 1q, a region that is frequently amplified in NSCLC⁴⁷ and associated with increased tumor recurrence⁴⁸. Together with our other data, this prompted us to examine expression patterns of these genes in clinical specimens of NSCLC. We found that the majority of clinical NSCLC samples expressed higher levels of *SKN* in malignant tissue than in matched normal one, implying a critical role for SKN in lung tumorigenesis. *DISP-1* expression was increased in a smaller subset of lung tumors. Interestingly, *DISP-1*, but not *SKN*, expression correlates with decreased overall and recurrence free survival, suggesting that in situations where *SKN* is overexpressed release of the processed ligand may be a rate-limiting step in HH-dependent tumors.

The role HH plays in human cancer has been controversial. Initially, results gained from the study of inherited forms of *PTCH-1* deletions, and from a variety of mouse models engineered to lack *PTCH-1*, implicated basal cell carcinoma (BCC), medulloblastoma and rhabdomyosarcoma as the predominant HH pathway dependent tumors^{49–54}. This work was further supported by the identification of *PTCH-1* or *SMO* mutations in sporadic forms of these tumors^{55,56}. It was later shown that the HH signaling pathway, as well as the ligands themselves, were enriched in numerous other types of human cancer^{57–63}. Furthermore, the viability of cells derived from these cancers was reduced *in vitro* when treated with SMO antagonists^{36,64,65}. Where examined, no mutations in the common components of the HH signaling pathway were found in these HH-ligand dependent cancers^{57–63}. Such results suggested that the HH-dependent tumor cell lines functioned, for the most part, in an autocrine-like manner, producing and responding to HH ligands themselves. It was later found that SMO antagonists could act non-specifically *in vitro*, and that *in vivo* HH secreted from tumor cells acted directly on the stroma to regulate tumor growth in a paracrine-like fashion⁶⁶. More rigorous *in vitro* analyses now indicate that the ability of HH to act in a paracrine or autocrine fashion may be context dependent^{31,67,68}. Our previous work revealed that some subset of NSCLC cells, human or mouse, produce and respond to HH ligands in an autocrine fashion^{31,33}. Such data were obtained using SMO inhibitors *in vitro* and using lentiviral mediated knockdown of numerous, distinct components of the HH signaling pathway. These results were further supported by immunohistochemistry analyses of primary human NSCLC samples, which showed SHH and GLI-1 enriching predominantly in epithelial tumor cells. Importantly, the localization of these proteins in primary NSCLC samples was further validated using *in situ* mRNA hybridization experiments. The work presented here is also consistent with a paracrine-like role for HH ligands in NSCLC, as a reduction in HH processing reduces the viability of NSCLC cells *in vitro* and *in vivo*.

Unfortunately, the paucity of antibodies to *SKN* or *DISP-1* capable of detecting these proteins in primary NSCLC specimens leaves us unable to complete further immunohistochemistry analyses. Even so, our results demonstrate the feasibility and potential benefit of targeting more proximal signaling elements within the HH pathway, and imply that similar therapeutic strategies could be explored to inhibit the growth of HH ligand-dependent cancers.

METHODS

NSCLC cell lines A549: human alveolar adenocarcinoma (squamous in nature), HOP62: human lung adenocarcinoma, H23: human lung adenocarcinoma (epithelial morphology), H522: human lung adenocarcinoma (epithelial morphology) and U1752: squamous bronchiolar epithelial were obtained and cultured as previously described³². ED-1: mouse lung adenocarcinoma^{33,37}, derived from the lung tumors of transgenic mice that express *CYCLIN-E* driven by the human *SURFACTANT-C* promoter, SHH-Light2³⁵, SHH-I³⁶ and HEK cells (293T or Bosc23)⁶⁹ were maintained as described. All expression constructs were in the pcDNA3.1 vector. The WT human *SHH* expression vector was a gift from Dr. Cliff Tabin. The *SKN* and *SKN-MYC-HIS* constructs were cloned from human cDNA (H23 cells) and were validated by sequencing. All lentiviral shRNA constructs are in the pLKO.1 vector and were either purchased from Open Biosystems, or engineered into the pLKO.1 TRC cloning vector directly⁷⁰. Lentivirus was packaged as per manufacturer's instructions (Open Biosystems) and cells were transduced as previously described³¹. All plasmids were transfected using Lipofectamine 2000 (Invitrogen) as per manufacturer's instructions.

Assays

HEK cells were transfected with plasmids expressing *wtSHH* or *SHHC24S* and *SKN*, and SHH palmitoylation assayed by [9,10-³H] palmitic acid (Perkin Elmer) incorporation as previously described⁶⁹. Conditioned medium (CM) activity was assayed by SHH-Light2 cell assay as before^{71,72} as a measure of SHH activity, which is normalized to SHH expression in the CM (determined by immunoblot) to determine SHH potency. Immunoprecipitations were performed as described⁷³, and levels of the indicated proteins were determined by immunoblot analysis⁷². The expression of the indicated genes was measured by quantitative real-time PCR (qRT-PCR) as described³⁹. NSCLC cells were transduced with shRNA, and 5 days later cell number was measured in two independent assays. Cell viability was assessed by monitoring ATP concentrations using the Cell Titer-Glo (CTG) assay (Promega) according to manufacturer's instructions (except for ED1 cells, which were assayed as described)⁷⁴, or by monitoring mitochondrial activity by the reduction of 3-(4,5-dimethyl-2-thiazolyl) 2,5-diphenyl-2H-tetrazolium bromide (MTT) to Formazan as before⁷⁵. Proliferation was assessed by incubating cells with 10 μ M BrdU (BD) for 4 hours, and immunostaining was performed as previously described⁷⁶. At least 6 independent fields were counted per experimental condition under the 20 \times objective of an Olympus IX71 microscope. Cell death was assessed by measuring lactate dehydrogenase (LDH) activity using the Tox-7 *In Vitro* Toxicology Assay Kit (Sigma) as specified by the manufacturer. The ratio between released LDH in the CM and the total LDH was used as a measure of cell death, while the total LDH value is of cell proliferation. Clonal growth was assessed as described³⁹ with these following modifications: 24 hours post transduction with the indicated constructs, media was replaced with media containing 2.5 μ g/mL puromycin for 24 hours, at which point cells were trypsinized and plated in 100 mm dishes at a density of 500 cells/plate. Three weeks later colonies were stained with crystal violet and visible colonies were quantified. In order to rescue growth defects resulted from decreased HH processing, NSCLC cells transduced with control, *SKN* or *DISP-1* specific shRNA were supplemented with either dual lipid modified SHH (purified from SHH-I cells³⁶ in a 0.1 %

NP-40 buffer) at a final concentration of 2.5 nM or purification buffer alone (final NP-40 concentration in media was 0.0003 %), and was replaced every 2–3 days. Alternatively, cells were treated with 15 μ M of the SMO agonist purmorphamine or vehicle control (DMSO). Cell viability was assessed by MTT assay 5 or 4 days, respectively, post transduction.

Antibodies

3 New Zealand barrier bred rabbits were injected with a SKN specific KLH-conjugated antigenic peptide: KVSREHEEELDQFELETDTLFG. Test bleeds were analyzed by ELISA, and the terminal bleeds from the best two rabbits were affinity purified to yield two polyclonal rabbit anti-SKN antibodies: SKN2883 and SKN2884. For DISP-1 antibody production this same protocol was followed to purify the DISP-Q5253 polyclonal antibody. The immunogenic sequence used for DISP-1 was the following: VEGFVHPITHIHHCPLQGRVKPAGMQNSLPRNFFLHPVQHIQAQEKIGKTNVHSLQRSIEEHLPKMAEPSSFVCRSTGSLKTCDDPENKQRELCKNRDVSNLESSGGTENKAGGKVELSLSQTDASVNSEHFNQNEPKVLFNHLMGEA. Antibodies for SKN were tested by immunoblotting lysates from HEK cells transfected with either pcDNA3.1 empty vector or a plasmid expressing *SKN-MYC-HIS* (Supplemental Figure S1a, b), and by immunoblotting (using SKN2884) SKN2883 immunoprecipitates from the lysates of H23 cells transduced with a Scramble control or 4 different *SKN* specific shRNA (Figure 1c). The antibody for DISP-1 was tested by immunoblotting lysates of A549 (Figure 4c) and H23 cells (Supplemental Figure S1c) transduced with shScramble and shGFP as controls, as well as 4 different *DISP-1* specific shRNA. The GLI-1 antibody was custom made by a contract laboratory³⁹. Commercially available antibodies used were: SHH (H-160) and α -TUBULIN (Santa Cruz), GAPDH (Ambion), BrdU, Cleaved CASPASE-3 and CYCLIN-D1 (Cell Signaling), MYC (9e10, Covance) and appropriate HRP or Alexa Fluor conjugated secondary antibodies (Invitrogen).

In vivo Experiments

All mouse work was conducted in accordance with protocols approved by the Institutional Animal Care and Use Committee (IACUC) at the university where it was performed. GFP positive ED1 cells were selected with 2.5 μ g/mL puromycin to stably express the indicated shRNA then injected into the tail vein of syngeneic FVB mice and tumor formation assessed as described³⁷. A549 xenografts were performed as previously described³¹ with the following modifications: for the shSKN xenografts 1.25×10^6 cells were injected, and for the shDISP xenografts 1×10^6 cells were injected.

Clinical expression and survival studies

Clinical expression of *SKN* and *DISP-1* was assessed in three different ways: A commercially available tumor cDNA array consisting of 24 matched pairs of human lung tumor and normal tissues was purchased and used per manufacturer's instructions (TissueScan Lung Cancer cDNA Array IV, Origene Technologies), 6 pairs of locally obtained matched pairs of human lung tumor and normal tissue were analyzed by qRT-PCR, and a set of 58 tumor/normal pairs from NSCLC patients was analyzed using a custom Agilent Whole Genome Oligonucleotide micro-array as previously described⁴³. Gene expression and patient survival data for two independent tumor datasets (Accession Numbers GSE8894 and GSE10245) were obtained from the *Gene Expression Omnibus* (<http://www.ncbi.nlm.nih.gov/geo/>) and normalized using GCRMA⁷⁷. GSE8894 consists of 138 post resection NSCLC tumors with information on recurrence-free survival⁷⁸, while GSE10245 consists of 58 high grade NSCLC tumors with both recurrence-free and overall survival data⁷⁹. The gene expression values used here were determined from array data, using the standard Affymetrix U133 Plus 2.0 protocol (data were pre-processed using GCRMA normalization). For each dataset, patients were grouped into tertiles based on

expression levels (i.e. low, middle and high) of *SKN* (probeset ID = 219687_at) or *DISP-1* (probeset ID = 228184_at), and survival times of patients with expression values in the lowest tertile compared to those of patients whose expression was ranked in the highest tertile. The tertile cutoff was chosen as approximately 33 % of patients tested, which showed increased expression of *DISP-1* in tumor vs normal tissue.

Statistical analysis

Results shown represent the mean of at least three independent experiments \pm standard error of the mean (SEM), unless otherwise noted. For the micro-array data, normalized \log_{10} expression values for each probe were compared between the normal and tumor samples using a two-tailed Wilcoxon matched-pairs sign rank test. Significance was tested using an unpaired one-tailed Student's t-test, except for the Kaplan-Meier survival curves, which were tested by a Mantel-Cox test. Differences were considered significant in the following way: * p 0.05, ** p 0.01, *** p 0.001.

Supplementary Material

Refer to Web version on PubMed Central for supplementary material.

Acknowledgments

Work was supported by NIH grants GM64011 (D.J. Robbins), R03-CA132166 (E. Dmitrovsky), R01-CA087546 (E. Dmitrovsky) and R01-CA111422 (E. Dmitrovsky); grants from the Samuel Waxman Cancer Research Foundation (E. Dmitrovsky, A. Capobianco); FICYT-POST10-27 (J. Rodriguez-Blanco) and from the American Lung Association/LUNGevity Foundation (D.J. Robbins). E. Dmitrovsky is an American Cancer Society Professor supported by a generous gift from the FM Kirby Foundation

REFERENCES

- Ingham PW, McMahon AP. Hedgehog signaling in animal development: paradigms and principles. *Genes Dev.* 2001; 15:3059–3087. [PubMed: 11731473]
- Farzan SF, Singh S, Schilling NS, Robbins DJ. The adventures of sonic hedgehog in development and repair. III. Hedgehog processing and biological activity. *Am J Physiol Gastrointest Liver Physiol.* 2008; 294:G844–G849. [PubMed: 18239057]
- Teglund S, Toftgård R. Hedgehog beyond medulloblastoma and basal cell carcinoma. *Biochim. Biophys. Acta.* 2010; 1805:181–208. [PubMed: 20085802]
- Yang L, Xie G, Fan Q, Xie J. Activation of the hedgehog-signaling pathway in human cancer and the clinical implications. *Oncogene.* 2010; 29:469–481. [PubMed: 19935712]
- Stone DM, Hynes M, Armanini M, Swanson TA, Gu Q, Johnson RL, et al. The tumour-suppressor gene patched encodes a candidate receptor for Sonic hedgehog. *Nature.* 1996; 384:129–134. [PubMed: 8906787]
- Marigo V, Davey RA, Zuo Y, Cunningham JM, Tabin CJ. Biochemical evidence that patched is the Hedgehog receptor. *Nature.* 1996; 384:176–179. [PubMed: 8906794]
- Chen Y, Struhl G. Dual roles for patched in sequestering and transducing Hedgehog. *Cell.* 1996; 87:553–563. [PubMed: 8898207]
- Quirk J, van den Heuvel M, Henrique D, Marigo V, Jones TA, Tabin C, et al. The smoothed gene and hedgehog signal transduction in *Drosophila* and vertebrate development. *Cold Spring Harb. Symp. Quant. Biol.* 1997; 62:217–226. [PubMed: 9598354]
- Stecca B, Ruiz i Altaba A. Context-dependent regulation of the GLI code in cancer by HEDGEHOG and non-HEDGEHOG signals. *J Mol Cell Biol.* 2010; 2:84–95. [PubMed: 20083481]
- Hoff Von DD, LoRusso PM, Rudin CM, Reddy JC, Yauch RL, Tibes R, et al. Inhibition of the hedgehog pathway in advanced basal-cell carcinoma. *N. Engl. J. Med.* 2009; 361:1164–1172. [PubMed: 19726763]

11. Rudin CM, Hann CL, Laterra J, Yauch RL, Callahan CA, Fu L, et al. Treatment of medulloblastoma with hedgehog pathway inhibitor GDC-0449. *N. Engl. J. Med.* 2009; 361:1173–1178. [PubMed: 19726761]
12. Low JA, de Sauvage FJ. Clinical experience with Hedgehog pathway inhibitors. *J. Clin. Oncol.* 2010; 28:5321–5326. [PubMed: 21041712]
13. Yauch RL, Dijkgraaf GJP, Alicke B, Januario T, Ahn CP, Holcomb T, et al. Smoothened mutation confers resistance to a Hedgehog pathway inhibitor in medulloblastoma. *Science.* 2009; 326:572–574. [PubMed: 19726788]
14. Dijkgraaf GJP, Alicke B, Weinmann L, Januario T, West K, Modrusan Z, et al. Small molecule inhibition of GDC-0449 refractory smoothened mutants and downstream mechanisms of drug resistance. *Cancer Res.* 2011; 71:435–444. [PubMed: 21123452]
15. Mann RK, Beachy PA. Novel lipid modifications of secreted protein signals. *Annu. Rev. Biochem.* 2004; 73:891–923. [PubMed: 15189162]
16. Porter JA, Young KE, Beachy PA. Cholesterol modification of hedgehog signaling proteins in animal development. *Science.* 1996; 274:255–259. [PubMed: 8824192]
17. Pepinsky RB, Zeng C, Wen D, Rayhorn P, Baker DP, Williams KP, et al. Identification of a palmitic acid-modified form of human Sonic hedgehog. *J Biol Chem.* 1998; 273:14037–14045. [PubMed: 9593755]
18. Chamoun Z, Mann RK, Nellen D, Kessler von DP, Bellotto M, Beachy PA, et al. Skinny hedgehog, an acyltransferase required for palmitoylation and activity of the hedgehog signal. *Science.* 2001; 293:2080–2084. [PubMed: 11486055]
19. Lee JD, Treisman JE. Sightless has homology to transmembrane acyltransferases and is required to generate active Hedgehog protein. *Curr Biol.* 2001; 11:1147–1152. [PubMed: 11509241]
20. Amanai K, Jiang J. Distinct roles of Central missing and Dispatched in sending the Hedgehog signal. *Development.* 2001; 128:5119–5127. [PubMed: 11748147]
21. Micchelli CA, The I, Selva E, Mogila V, Perrimon N. Rasp, a putative transmembrane acyltransferase, is required for Hedgehog signaling. *Development.* 2002; 129:843–851. [PubMed: 11861468]
22. Buglino JA, Resh MD. Hhat is a palmitoylacyltransferase with specificity for N-palmitoylation of Sonic Hedgehog. *J Biol Chem.* 2008; 283:22076–22088. [PubMed: 18534984]
23. Taylor FR, Wen D, Garber EA, Carmillo AN, Baker DP, Arduini RM, et al. Enhanced potency of human Sonic hedgehog by hydrophobic modification. *Biochemistry.* 2001; 40:4359–4371. [PubMed: 11284692]
24. Kohtz JD, Lee HY, Gaiano N, Segal J, Ng E, Larson T, et al. N-terminal fatty-acylation of sonic hedgehog enhances the induction of rodent ventral forebrain neurons. *Development.* 2001; 128:2351–2363. [PubMed: 11493554]
25. Burke R, Nellen D, Bellotto M, Hafen E, Senti KA, Dickson BJ, et al. Dispatched, a novel sterol-sensing domain protein dedicated to the release of cholesterol-modified hedgehog from signaling cells. *Cell.* 1999; 99:803–815. [PubMed: 10619433]
26. Caspary T, Garcia-García MJ, Huangfu D, Eggenschwiler JT, Wyler MR, Rakeman AS, et al. Mouse Dispatched homolog1 is required for long-range, but not juxtacrine, Hh signaling. *Curr Biol.* 2002; 12:1628–1632. [PubMed: 12372258]
27. Ma Y, Erkner A, Gong R, Yao S, Taipale J, Basler K, et al. Hedgehog-mediated patterning of the mammalian embryo requires transporter-like function of dispatched. *Cell.* 2002; 111:63–75. [PubMed: 12372301]
28. Kawakami T, Kawcak T, Li Y-J, Zhang W, Hu Y, Chuang P-T. Mouse dispatched mutants fail to distribute hedgehog proteins and are defective in hedgehog signaling. *Development.* 2002; 129:5753–5765. [PubMed: 12421714]
29. Chen M-H, Li Y-J, Kawakami T, Xu S-M, Chuang P-T. Palmitoylation is required for the production of a soluble multimeric Hedgehog protein complex and long-range signaling in vertebrates. *Genes Dev.* 2004; 18:641–659. [PubMed: 15075292]
30. Zhang XM, Ramalho-Santos M, McMahon AP. Smoothened mutants reveal redundant roles for Shh and Ihh signaling including regulation of L/R asymmetry by the mouse node. *Cell.* 2001; 105:781–792. [PubMed: 11440720]

31. Singh S, Wang Z, Liang Fei D, Black KE, Goetz JA, Tokhunts R, et al. Hedgehog-Producing Cancer Cells Respond to and Require Autocrine Hedgehog Activity. *Cancer Res.* 2011; 71:4454–4463. [PubMed: 21565978]
32. Yuan Z, Goetz JA, Singh S, Ogden SK, Petty WJ, Black CC, et al. Frequent requirement of hedgehog signaling in non-small cell lung carcinoma. *Oncogene.* 2007; 26:1046–1055. [PubMed: 16909105]
33. Ma Y, Fiering S, Black C, Liu X, Yuan Z, Memoli VA, et al. Transgenic cyclin E triggers dysplasia and multiple pulmonary adenocarcinomas. *Proc Natl Acad Sci USA.* 2007; 104:4089–4094. [PubMed: 17360482]
34. Gialmanidis IP, Bravou V, Amanetopoulou SG, Varakis J, Kourea H, Papadaki H. Overexpression of hedgehog pathway molecules and FOXM1 in non-small cell lung carcinomas. *Lung Cancer.* 2009; 66:64–74. [PubMed: 19200615]
35. Chen JK, Taipale J, Young KE, Maiti T, Beachy PA. Small molecule modulation of Smoothed activity. *Proc Natl Acad Sci USA.* 2002; 99:14071–14076. [PubMed: 12391318]
36. Cooper MK, Porter JA, Young KE, Beachy PA. Teratogen-mediated inhibition of target tissue response to Shh signaling. *Science.* 1998; 280:1603–1607. [PubMed: 9616123]
37. Liu X, Sempere LF, Galimberti F, Freemantle SJ, Black C, Dragnev KH, et al. Uncovering growth-suppressive MicroRNAs in lung cancer. *Clin Cancer Res.* 2009; 15:1177–1183. [PubMed: 19228723]
38. Legrand C, Bour JM, Jacob C, Capiaumont J, Martial A, Marc A, et al. Lactate dehydrogenase (LDH) activity of the cultured eukaryotic cells as marker of the number of dead cells in the medium [corrected]. *J. Biotechnol.* 1992; 25:231–243. [PubMed: 1368802]
39. Fei DL, Li H, Kozul CD, Black KE, Singh S, Gosse JA, et al. Activation of Hedgehog signaling by the environmental toxicant arsenic may contribute to the etiology of arsenic-induced tumors. *Cancer Res.* 2010; 70:1981–1988. [PubMed: 20179202]
40. Katoh Y, Katoh M. Hedgehog target genes: mechanisms of carcinogenesis induced by aberrant hedgehog signaling activation. *Curr. Mol. Med.* 2009; 9:873–886. [PubMed: 19860666]
41. Miura GI, Buglino J, Alvarado D, Lemmon MA, Resh MD, Treisman JE. Palmitoylation of the EGFR ligand Spitz by Rasp increases Spitz activity by restricting its diffusion. *Dev Cell.* 2006; 10:167–176. [PubMed: 16459296]
42. Sinha S, Chen JK. Purmorphamine activates the Hedgehog pathway by targeting Smoothed. *Nat Chem Biol.* 2006; 2:29–30. [PubMed: 16408088]
43. Lockwood WW, Chari R, Coe BP, Thu KL, Garnis C, Malloff CA, et al. Integrative Genomic Analyses Identify BRF2 as a Novel Lineage-Specific Oncogene in Lung Squamous Cell Carcinoma. *Plos Med.* 2010; 7 –.
44. Neal JW, Sequist LV. Exciting new targets in lung cancer therapy: ALK, IGF-1R, HDAC, and Hh. *Curr Treat Options Oncol.* 2010; 11:36–44. [PubMed: 20676809]
45. Lauth M, Bergström A, Shimokawa T, Toftgård R. Inhibition of GLI-mediated transcription and tumor cell growth by small-molecule antagonists. *Proc Natl Acad Sci USA.* 2007; 104:8455–8460. [PubMed: 17494766]
46. Ng JMY, Curran T. The Hedgehog's tale: developing strategies for targeting cancer. *Nat. Rev. Cancer.* 2011; 11:493–501. [PubMed: 21614026]
47. Petersen I, Bujard M, Petersen S, Wolf G, Goeze A, Schwendel A, et al. Patterns of chromosomal imbalances in adenocarcinoma and squamous cell carcinoma of the lung. *Cancer Res.* 1997; 57:2331–2335. [PubMed: 9192802]
48. Tai ALS, Yan W-S, Fang Y, Xie D, Sham JST, Guan X-Y. Recurrent chromosomal imbalances in nonsmall cell lung carcinoma: the association between 1q amplification and tumor recurrence. *Cancer.* 2004; 100:1918–1927. [PubMed: 15112273]
49. Johnson RL, Rothman AL, Xie J, Goodrich LV, Bare JW, Bonifas JM, et al. Human homolog of patched, a candidate gene for the basal cell nevus syndrome. *Science.* 1996; 272:1668–1671. [PubMed: 8658145]
50. Hahn H, Wicking C, Zaphiropoulos PG, Gailani MR, Shanley S, Chidambaram A, et al. Mutations of the human homolog of *Drosophila* patched in the nevoid basal cell carcinoma syndrome. *Cell.* 1996; 85:841–851. [PubMed: 8681379]

51. Xie J, Johnson RL, Zhang X, Bare JW, Waldman FM, Cogen PH, et al. Mutations of the PATCHED gene in several types of sporadic extracutaneous tumors. *Cancer Res.* 1997; 57:2369–2372. [PubMed: 9192811]
52. Goodrich LV, Milenkovic L, Higgins KM, Scott MP. Altered neural cell fates and medulloblastoma in mouse patched mutants. *Science.* 1997; 277:1109–1113. [PubMed: 9262482]
53. Adolphe C, Hetherington R, Ellis T, Wainwright B. Patched1 functions as a gatekeeper by promoting cell cycle progression. *Cancer Res.* 2006; 66:2081–2088. [PubMed: 16489008]
54. Tostar U, Malm CJ, Meis-Kindblom JM, Kindblom L-G, Toftgård R, Undén AB. Deregulation of the hedgehog signalling pathway: a possible role for the PTCH and SUFU genes in human rhabdomyoma and rhabdomyosarcoma development. *J. Pathol.* 2006; 208:17–25. [PubMed: 16294371]
55. Shen T, Park WS, Böni R, Saini N, Pham T, Lash AE, et al. Detection of loss of heterozygosity on chromosome 9q22.3 in microdissected sporadic basal cell carcinoma. *Hum. Pathol.* 1999; 30:284–287. [PubMed: 10088546]
56. Xie J, Murone M, Luoh SM, Ryan A, Gu Q, Zhang C, et al. Activating Smoothed mutations in sporadic basal-cell carcinoma. *Nature.* 1998; 391:90–92. [PubMed: 9422511]
57. Kubo M, Nakamura M, Tasaki A, Yamanaka N, Nakashima H, Nomura M, et al. Hedgehog signaling pathway is a new therapeutic target for patients with breast cancer. *Cancer Res.* 2004; 64:6071–6074. [PubMed: 15342389]
58. Thayer SP, di Magliano MP, Heiser PW, Nielsen CM, Roberts DJ, Lauwers GY, et al. Hedgehog is an early and late mediator of pancreatic cancer tumorigenesis. *Nature.* 2003; 425:851–856. [PubMed: 14520413]
59. Berman DM, Karhadkar SS, Maitra A, Montes De Oca R, Gerstenblith MR, Briggs K, et al. Widespread requirement for Hedgehog ligand stimulation in growth of digestive tract tumours. *Nature.* 2003; 425:846–851. [PubMed: 14520411]
60. Watkins DN, Berman DM, Burkholder SG, Wang B, Beachy PA, Baylin SB. Hedgehog signalling within airway epithelial progenitors and in small-cell lung cancer. *Nature.* 2003; 422:313–317. [PubMed: 12629553]
61. Clement V, Sanchez P, de Tribolet N, Radovanovic I, Ruiz i Altaba A. HEDGEHOG-GLI1 signaling regulates human glioma growth, cancer stem cell self-renewal, and tumorigenicity. *Curr Biol.* 2007; 17:165–172. [PubMed: 17196391]
62. Karhadkar SS, Bova GS, Abdallah N, Dhara S, Gardner D, Maitra A, et al. Hedgehog signalling in prostate regeneration, neoplasia and metastasis. *Nature.* 2004; 431:707–712. [PubMed: 15361885]
63. Sanchez P, Hernández AM, Stecca B, Kahler AJ, DeGueme AM, Barrett A, et al. Inhibition of prostate cancer proliferation by interference with SONIC HEDGEHOG-GLI1 signaling. *Proc Natl Acad Sci USA.* 2004; 101:12561–12566. [PubMed: 15314219]
64. Mas C, Ruiz i Altaba A. Small molecule modulation of HH-GLI signaling: current leads, trials and tribulations. *Biochem. Pharmacol.* 2010; 80:712–723. [PubMed: 20412786]
65. Stanton BZ, Peng LF. Small-molecule modulators of the Sonic Hedgehog signaling pathway. *Mol Biosyst.* 2010; 6:44–54. [PubMed: 20024066]
66. Yauch RL, Gould SE, Scales SJ, Tang T, Tian H, Ahn CP, et al. A paracrine requirement for hedgehog signalling in cancer. *Nature.* 2008; 455:406–410. [PubMed: 18754008]
67. Lauth M, Bergström A, Shimokawa T, Tostar U, Jin Q, Fendrich V, et al. DYRK1B-dependent autocrine-to-paracrine shift of Hedgehog signaling by mutant RAS. *Nat. Struct. Mol. Biol.* 2010; 17:718–725. [PubMed: 20512148]
68. Park K-S, Martelotto LG, Peifer M, Sos ML, Karnezis AN, Mahjoub MR, et al. A crucial requirement for Hedgehog signaling in small cell lung cancer. *Nat Med.* 2011
69. Singh S, Tokhunts R, Baubet V, Goetz JA, Huang ZJ, Schilling NS, et al. Sonic hedgehog mutations identified in holoprosencephaly patients can act in a dominant negative manner. *Hum. Genet.* 2009; 125:95–103. [PubMed: 19057928]
70. Moffat J, Grueneberg DA, Yang X, Kim SY, Kloepfer AM, Hinkle G, et al. A lentiviral RNAi library for human and mouse genes applied to an arrayed viral high-content screen. *Cell.* 2006; 124:1283–1298. [PubMed: 16564017]

71. Zeng X, Goetz JA, Suber LM, Scott WJ, Schreiner CM, Robbins DJ. A freely diffusible form of Sonic hedgehog mediates long-range signalling. *Nature*. 2001; 411:716–720. [PubMed: 11395778]
72. Goetz JA, Singh S, Suber LM, Kull FJ, Robbins DJ. A highly conserved amino-terminal region of sonic hedgehog is required for the formation of its freely diffusible multimeric form. *J Biol Chem*. 2006; 281:4087–4093. [PubMed: 16339763]
73. Robbins DJ, Nybakken KE, Kobayashi R, Sisson JC, Bishop JM, Théron PP. Hedgehog elicits signal transduction by means of a large complex containing the kinesin-related protein costal2. *Cell*. 1997; 90:225–234. [PubMed: 9244297]
74. Petty WJ, Li N, Biddle A, Bounds R, Nitkin C, Ma Y, et al. A novel retinoic acid receptor beta isoform and retinoid resistance in lung carcinogenesis. *J. Natl. Cancer Inst*. 2005; 97:1645–1651. [PubMed: 16288117]
75. Denizot F, Lang R. Rapid colorimetric assay for cell growth and survival. Modifications to the tetrazolium dye procedure giving improved sensitivity and reliability. *J. Immunol. Methods*. 1986; 89:271–277. [PubMed: 3486233]
76. Fernandez C, Tatard VM, Bertrand N, Dahmane N. Differential modulation of Sonic-hedgehog-induced cerebellar granule cell precursor proliferation by the IGF signaling network. *Dev. Neurosci*. 2010; 32:59–70. [PubMed: 20389077]
77. Wu Z, Irizarry R, Gentleman R, Martinez-Murillo F, Spencer F. A model-based background adjustment for oligonucleotide expression arrays. *J Am Stat Assoc*. 2004; 99:909–917.
78. Lee E-S, Son D-S, Kim S-H, Lee J, Jo J, Han J, et al. Prediction of recurrence-free survival in postoperative non-small cell lung cancer patients by using an integrated model of clinical information and gene expression. *Clin Cancer Res*. 2008; 14:7397–7404. [PubMed: 19010856]
79. Kuner R, Muley T, Meister M, Ruschhaupt M, Buness A, Xu EC, et al. Global gene expression analysis reveals specific patterns of cell junctions in non-small cell lung cancer subtypes. *Lung Cancer*. 2009; 63:32–38. [PubMed: 18486272]

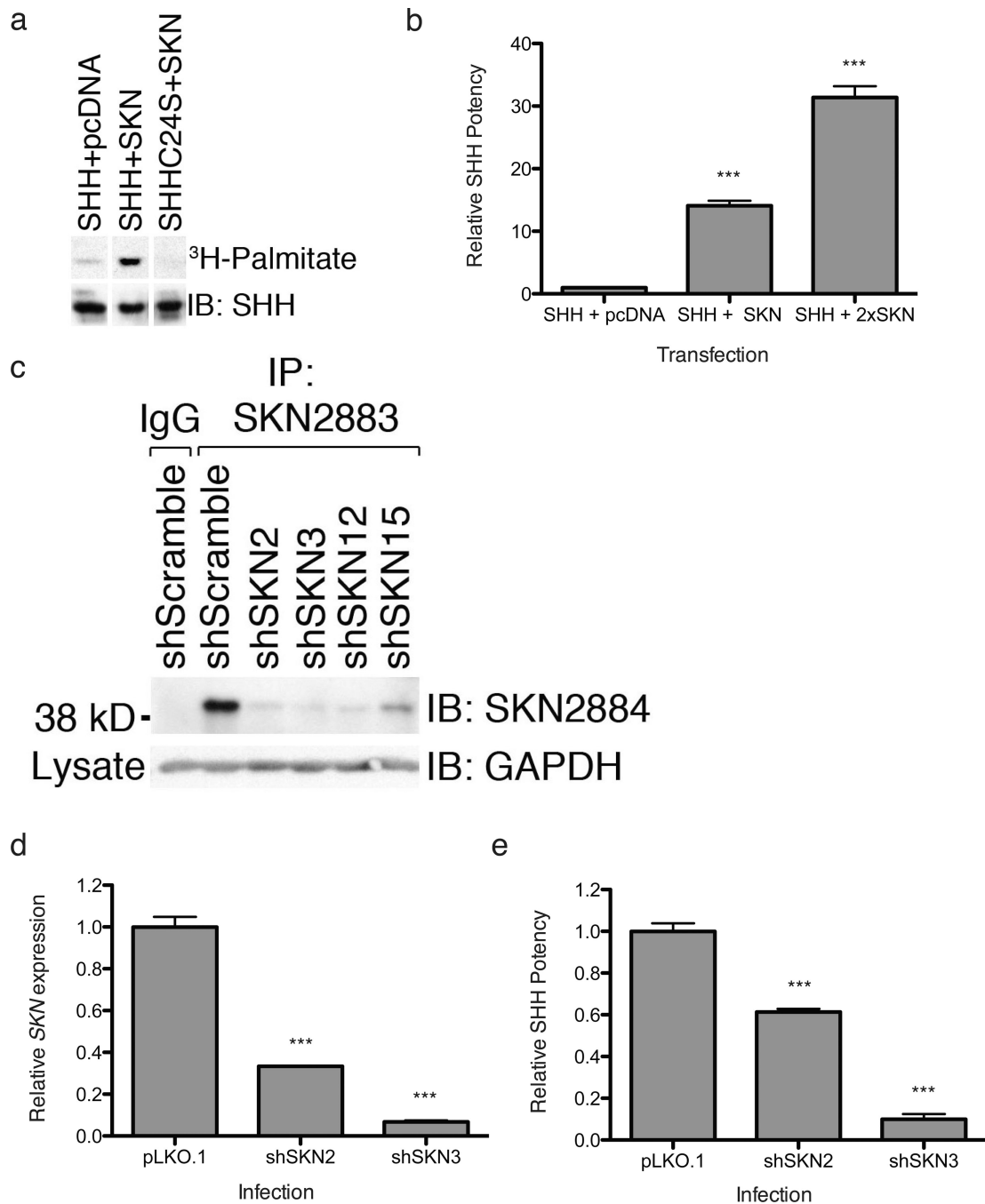


Figure 1. The Hedgehog acyl-transferase SKN regulates HH activity

a, *SKN* overexpression increased the palmitoylation of wtSHH, but not a mutated form, SHHC24S, in which the acceptor Cysteine was mutated to a Serine. HEK cells transfected with the indicated constructs were metabolically labeled with ³H-Palmitate. Lysates were collected and subjected to immunoprecipitation with an anti-SHH antibody. The same membrane was also immunoblotted (IB) with an anti-SHH antibody. **b**, Co-expression of *SKN* with *SHH* in HEK cells increased the potency of SHH in the conditioned media (CM). SHH potency was assessed by normalizing CM activity (SHH-Light2 cell assay) to the amount of SHH protein in the CM. Values were normalized to a pcDNA control. **c**, The

ability of 4 *SKN* specific shRNA to knockdown endogenous *SKN* was determined by transducing H23 cells with the indicated shRNAs. Lysates were collected and *SKN* was immunoprecipitated (IP) with an anti-*SKN* antibody (SKN2883) or rabbit IgG as a control. IPs were resolved by SDS-PAGE and visualized by immunoblotting (IB) using a second anti-*SKN* antibody (SKN2884). IB of input lysates with an anti-GAPDH antibody verified normalization. **d**, *SKN* was knocked down in SHH-I cells, which secrete high levels of active SHH, with the indicated shRNA and knockdown efficiency assessed by qRT-PCR. *GAPDH* expression was used as an internal control and results were normalized to a pLKO.1 control. **e**, This knockdown of *SKN* reduced the potency of SHH in the CM compared to a pLKO.1 empty vector control. Error bars represent SEM of 3 independent experiments. The asterisks (*) denote a statistically significant change (* p 0.05, ** p 0.01, *** p 0.001) vs. control (pcDNA or pLKO.1).

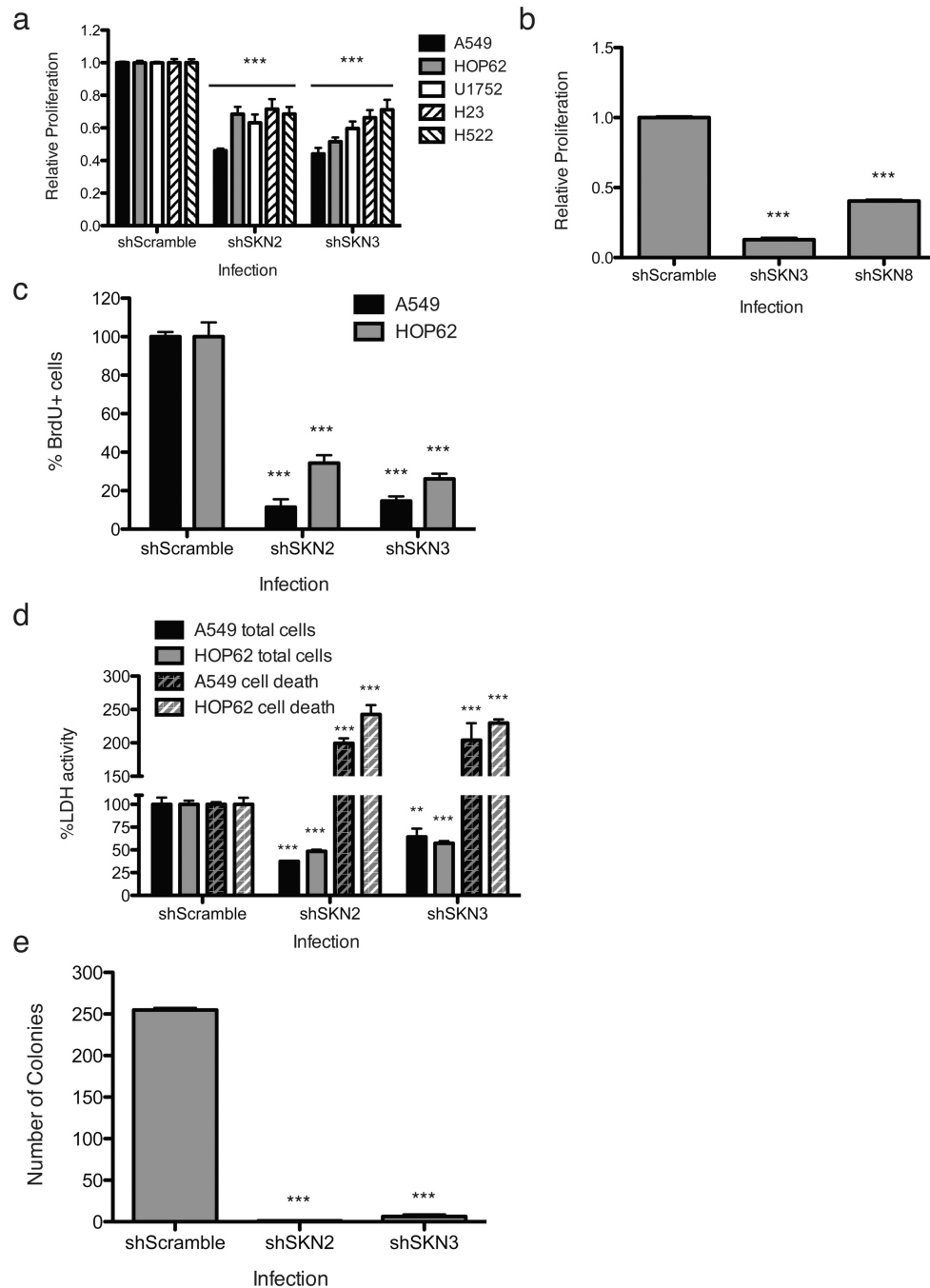


Figure 2. SKN is necessary for the proliferation of NSCLC cells *in vitro*

a, Knockdown of *SKN* reduced the proliferation of the indicated human NSCLC cell lines and **b**, ED1 cells, a mouse lung adenocarcinoma cell line. Cell number was assayed by a CTG assay 5 days post transduction with the indicated shRNA. Values were normalized to cells transduced with a shScramble control. **c**, Knockdown of *SKN* reduced the rate of proliferation of both A549 and HOP62 cells. Proliferative rates were assayed by staining for mitotic cells with BrdU 4 days post transduction with the indicated shRNA. BrdU positive cells were quantified and normalized to cells transduced with a shScramble control. A representative experiment is shown and error bars represent SEM of 6 different fields. **d**,

Knockdown of *SKN* induced cell death in both A549 and HOP62 cells. Five days post transduction with the indicated shRNA, cell death and number were assayed simultaneously using a Lactate Dehydrogenase (LDH) cytotoxicity assay. Released LDH divided by total LDH measures cell death, while total LDH measures total cell number. A representative experiment is shown and error bars represent SEM of 4 technical replicates. **e**, Knockdown of *SKN* reduced the colony forming capacity of A549 cells. Five hundred cells transduced with the indicated shRNA were plated in 100 mm dishes and allowed to grow for 3 weeks, at which point colonies were stained and quantified. Error bars represent SEM of 3 independent experiments, unless otherwise indicated. The asterisk (*) denotes a statistically significant change (* p 0.05, ** p 0.01, *** p 0.001) vs. control (shScramble).

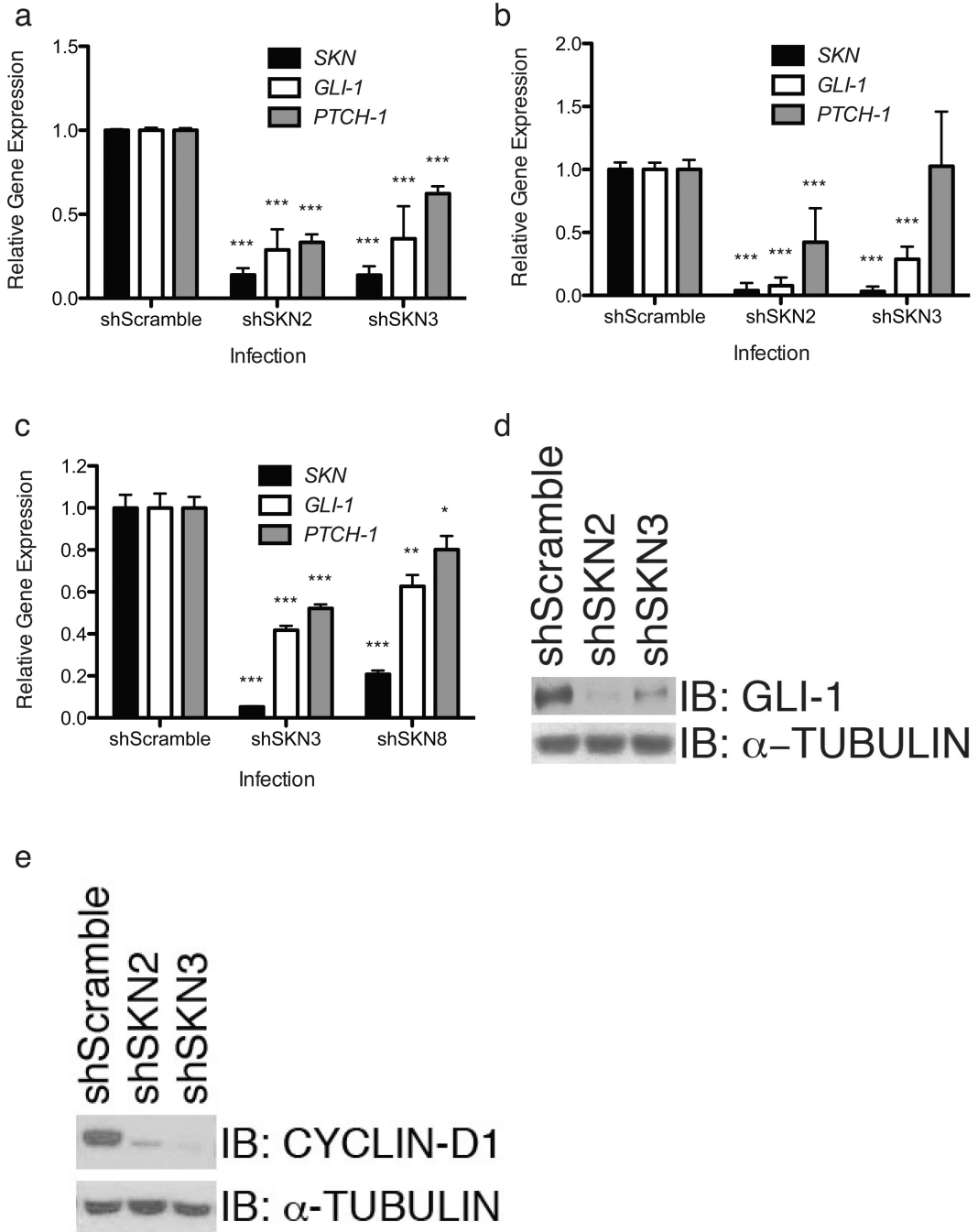


Figure 3. SKN is required for the activity of the HH pathway in NSCLC cells
a, Knockdown of *SKN* in A549 or **b**, HOP62 cells attenuated the expression of the HH target genes *GLI-1* and *PTCH-1*. Expression levels were assessed by qRT-PCR 3 days post transduction with the indicated shRNA. *GAPDH* expression was used as an internal control, and results are normalized to cells transduced with a shScramble control. **c**, HH target gene expression was reduced in polyclonal ED1 cells stably expressing the indicated shRNA. Cells were serum starved in media containing 0.5 % FBS for 24 hours prior to qRT-PCR analysis. **d**, Knockdown of *SKN* in A549 cells reduced the steady-state levels of the proteins *GLI-1* and **e**, *CYCLIN-D1*. Lysates from cells transduced with the indicated shRNA were

harvested 3 days post transduction, resolved by SDS-PAGE and immunoblotted (IB) with antibodies to GLI-1, CYCLIN-D1 or α -TUBULIN as a normalization control. Error bars represent SEM of 3 independent experiments. The asterisk (*) denotes a statistically significant change (* $p < 0.05$, ** $p < 0.01$, *** $p < 0.001$) vs. control (shScramble).

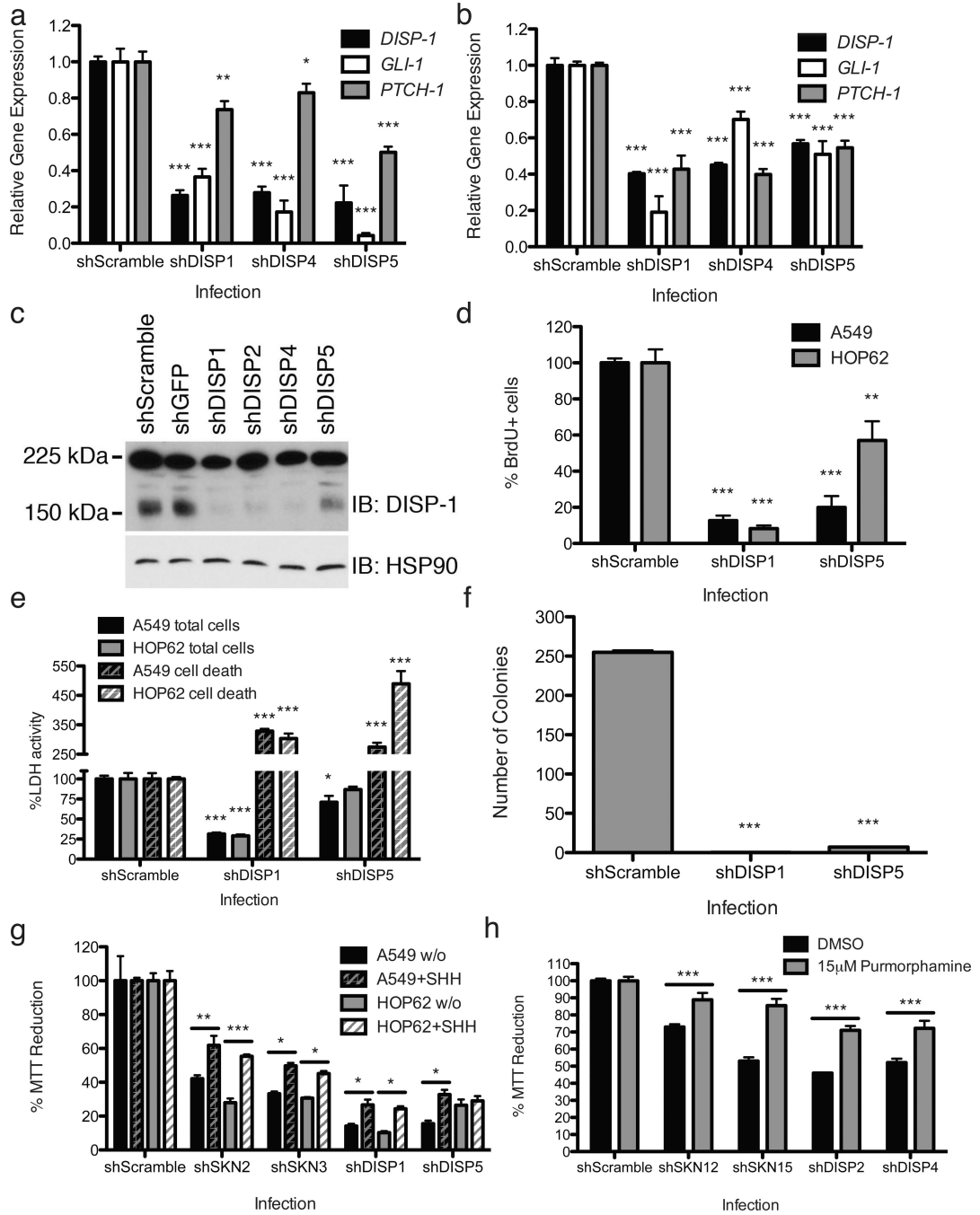


Figure 4. DISP-1, an additional regulator of HH processing, is required for NSCLC proliferation
a, Knockdown of *DISP-1* in A549 or **b**, HOP62 cells attenuated the expression of the HH target genes *GLI-1* and *PTCH-1*. Expression levels were assessed by qRT-PCR 3 days post transduction with the indicated shRNA. *GAPDH* expression was used as an internal control, and results are normalized to cells transduced with a shScramble control. **c**, The ability of 4 *DISP-1* specific shRNA to knockdown endogenous *DISP-1* was determined by transducing H23 cells with the indicated shRNAs. Lysates were collected and resolved by SDS-PAGE and visualized by immunoblotting (IB) using an anti-*DISP-1* antibody (DISP-Q5253). Heat Shock Protein-90 (HSP-90) was used as a normalization control. **d**, Knockdown of *DISP-1*

reduced the rate of proliferation of both A549 and HOP62 cells. Proliferative rates were assayed by staining for mitotic cells with BrdU 4 days post transduction with the indicated shRNA. BrdU positive cells were quantified and normalized to cells transduced with a shScramble control. A representative experiment is shown and error bars represent SEM of 6 different fields. **e**, Knockdown of *DISP-1* induced cell death in both A549 and HOP62 cells. 5 days post transduction with the indicated shRNA, cell death and number were assayed simultaneously using a LDH cytotoxicity assay. Released LDH divided by total LDH measures cell death, while total LDH measures total cell number. A representative experiment is shown and error bars represent SEM of 4 technical replicates. **f**, Knockdown of *DISP-1* reduced the colony forming capacity of A549 cells. Five hundred cells transduced with the indicated shRNA were plated in 100 mm dishes and allowed to grow for 3 weeks, at which point colonies were stained and quantified. **g**, Exogenous lipid modified SHH can partially rescue the proliferative defects of both A549 and HOP62 cells transduced with the indicated constructs. Cells were transduced with two *SKN* specific, two *DISP-1* specific or a scramble shRNA control. Twenty-four hours post transduction, viral media was substituted with fresh media containing purified lipid-modified SHH or SHH purification buffer at the same concentration. Four days later cell number was measured by MTT assay and normalized to the appropriate shScramble control. A representative experiment is shown and error bars represent SEM of 6 technical replicates. **h**, The SMO agonist purmorphamine can rescue the proliferative defects of A549 cells transduced with the indicated constructs. A549 cells were transduced with the indicated scramble, *SKN* or *DISP-1* shRNAs. Viral media was removed 24 h later and was substituted with fresh media containing either 15 μ M purmorphamine or vehicle (DMSO) control. Four days post transduction cell number was measured using a MTT assay and normalized to cells transduced with a shScramble control. A representative experiment is shown and error bars represent SEM of 6 technical replicates. Error bars represent SEM of 3 independent experiments (unless otherwise indicated). The asterisk (*) denotes a statistically significant change (* p 0.05, ** p 0.01, *** p 0.001) vs. control (shScramble unless otherwise indicated by a bar).

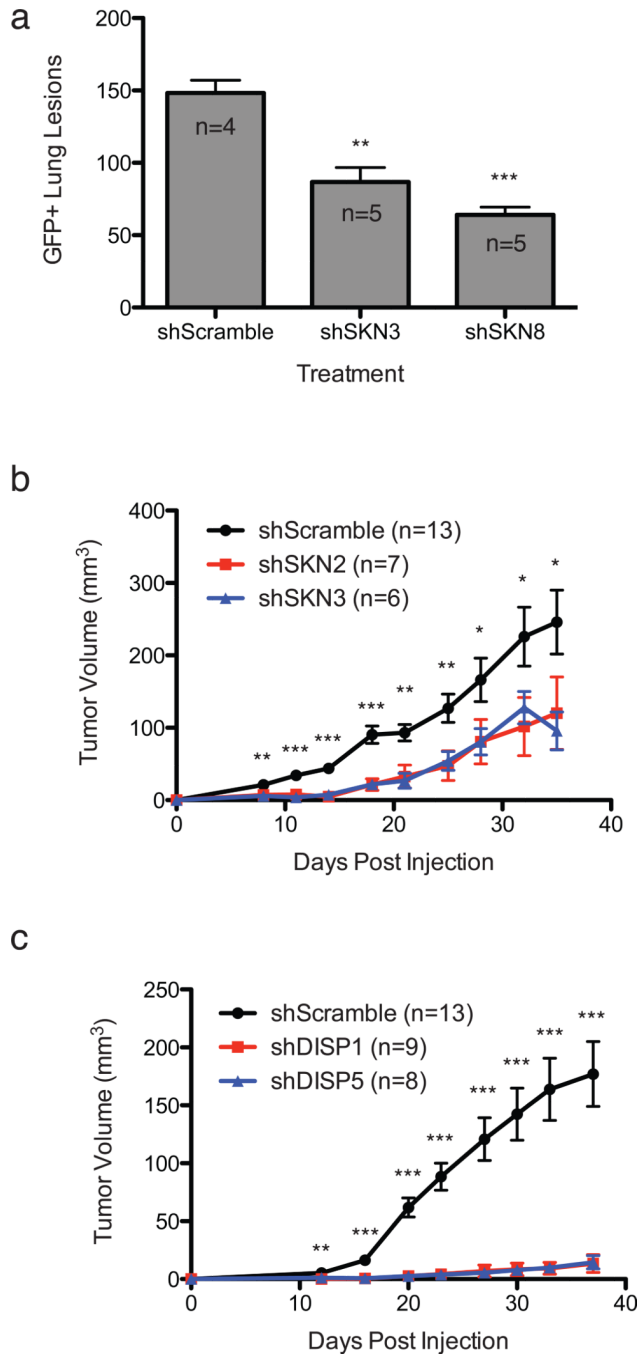


Figure 5. HH processing is required for NSCLC growth *in vivo*

a, Stable knockdown of *SKN* reduced tumor formation in a syngeneic mouse model of NSCLC. 8×10^5 GFP-positive, puromycin selected ED1 NSCLC cells expressing the indicated shRNA were injected into the tail-vein of syngeneic FVB mice (shScramble n=4, shSKN3 n=5, shSKN8 n=5). Four weeks later lungs were harvested, sectioned, stained for GFP expression, and lesions were quantified. **b**, Knockdown of *SKN* or **c**, *DISP-1* reduced the ability of A549 xenografts to grow in nude mice. 1.25×10^6 (for shSKN) and 1.00×10^6 (for shDISP) A549 cells transiently transduced with the indicated shRNAs were injected into the flanks of nude mice (shScramble n=13, shSKN2 n=7, shSKN3 n=6, shDISP n=9,

shDISP n=8) and tumor volume was measured biweekly. Error bars represent SEM. The asterisk (*) denotes a statistically significant change (* p 0.05, ** p 0.01, *** p 0.001) vs. control (shScramble).

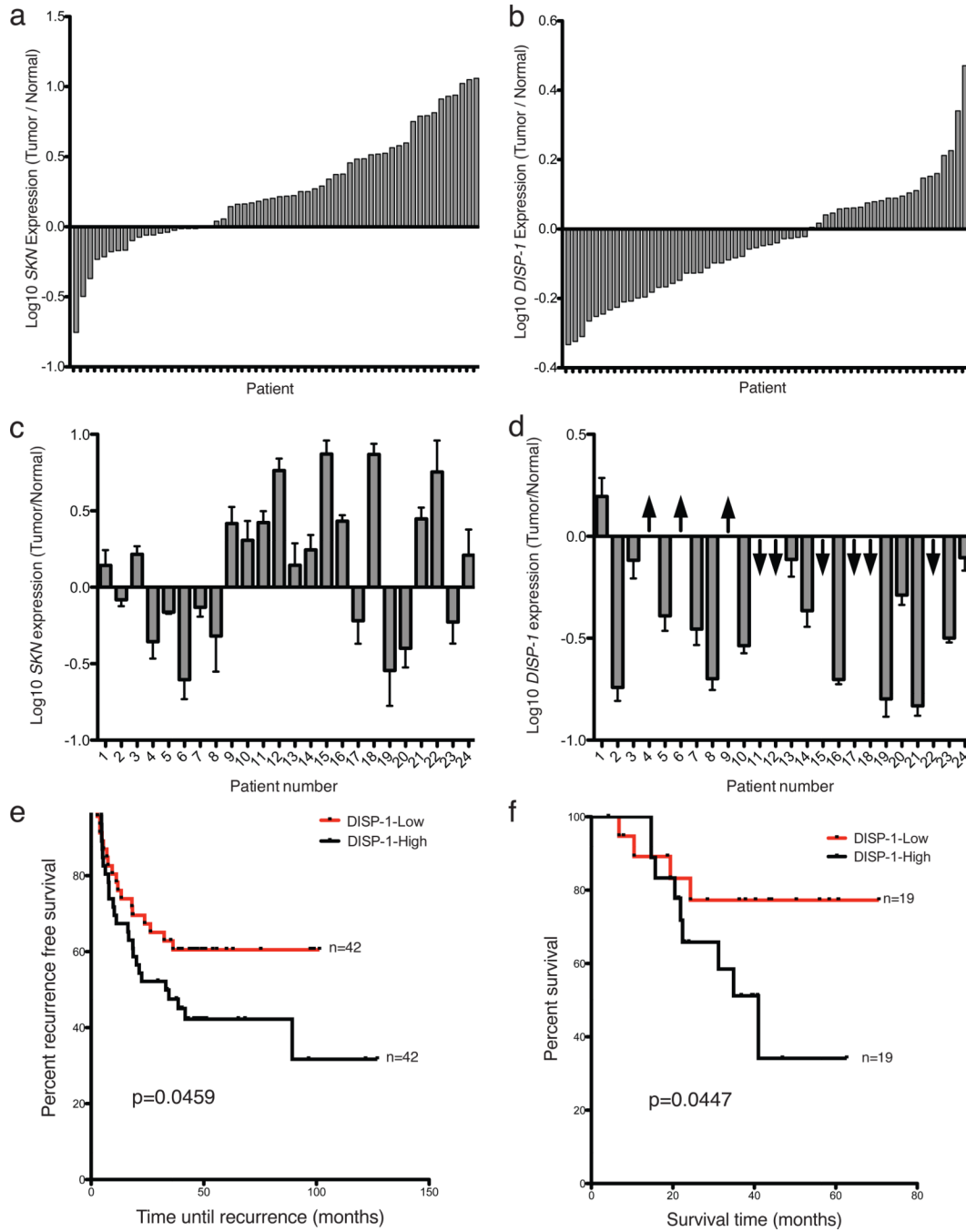


Figure 6. HH processing gene products are overexpressed in human NSCLCs and are associated with an unfavorable clinical outcome

a, *SKN* and **b**, *DISP-1* are differentially expressed in NSCLCs as compared to the corresponding matched normal lung tissue. Expression levels from 58 matched NSCLC/normal lung tissue pairs were assessed by oligonucleotide micro-array analyses. Gene expression in NSCLC was normalized to matched normal tissue and plotted as the Log₁₀ change (tumor/normal). **c**, *SKN* is overexpressed in commercially available clinical lung cancer specimens, confirming the pattern of expression detected by micro-array analysis. These were purchased from Origene (Tissuescan Lung Cancer cDNA Array IV) and consist of 24 matched lung cancer/normal lung cDNA pairs pre-normalized to *-ACTIN*. *SKN*

expression was determined by qRT-PCR, and lung tumor expression was normalized to matched normal control. **d**, *DISP-1* is differentially expressed in clinical lung cancer specimens. The same Tissuescan cDNA array was used to assess *DISP-1* levels by qRT-PCR. Arrows represent pairs where *DISP-1* expression was below the threshold of detection in either normal lung tissue (up arrow) or lung tumor (down arrow). **e**, Higher *DISP-1* expression is associated with reduced recurrence free survival. A publically available dataset (GSE8894) consisting of micro-array profiles of 138 NSCLC cases and an associated clinical survival database (recurrence-free survival) was mined to find correlations between *DISP-1* expression and recurrence free survival. Lung cancers were separated into tertiles based on *DISP-1* expression, and the top third compared to the bottom third. **f**, Higher *DISP-1* expression is associated with reduced survival in a second publically available dataset (GSE10245) consisting of micro-array profiles of 58 NSCLC cases and an associated clinical outcome database (overall and progression-free survival). This dataset was analyzed in the same manner as for GSE10245. P-values reported are from a one-tailed Log-rank (Mantel-Cox) test.